

Generalized Fried parameter after adaptive optics partial wave-front compensation

Manuel P. Cagigal and Vidal F. Canales

Departamento de Física Aplicada, Universidad de Cantabria, Los Castros S/N, 39005 Santander, Spain

Received July 12, 1999; revised December 22, 1999; accepted February 9, 2000

Atmospheric turbulence imposes the resolution limit attainable by large ground-based telescopes. This limit is λ/r_0 , where r_0 is the Fried parameter or seeing cell size. Working in the visible, adaptive optics systems can partially compensate for turbulence-induced distortions. By analogy with the Fried parameter, r_0 , we have introduced a generalized Fried parameter, ρ_0 , that plays the same role as r_0 but in partial compensation. Using this parameter and the residual phase variance, we have described the phase structure function, estimated the point-spread function halo size, and derived an expression for the Strehl ratio as a function of the degree of compensation. Finally, it is shown that ρ_0 represents the diameter of the coherent cells in the pupil domain. © 2000 Optical Society of America [S0740-3232(00)01605-7]

OCIS codes: 010.1080, 110.6770.

1. INTRODUCTION

Random aberrations on the pupil of the telescope due to atmospheric turbulence determine the angular resolution of ground-based telescopes. The compensation of the wave-front degradation before detection (adaptive optics) and the extraction of diffraction-limited information from the image series (speckle interferometry) are the two techniques able to overcome this limitation. The main advantage of adaptive optics systems is that they perform a real-time correction.¹⁻³ A wave-front sensor measures the instantaneous aberrations, and, using this information, a deformable mirror changes its shape to compensate for this distortion. Although adaptive optics systems with a large number of subapertures in the wave-front sensor and a large number of actuators in the deformable mirror provide the best results, they are complicated and expensive, and they stress current technology to its limit. In contrast, the use of simpler adaptive optics systems has great potential application. In this paper imaging with partially compensated adaptive optics systems (fewer than one actuator per atmospheric coherence diameter⁴⁻⁶) is analyzed.

We will consider that the correction system compensates pure Zernike polynomials. However, it is shown that the main results remain valid when a limited amount of noise affects the system performance. For systems based on curvature sensing, a straightforward application of the results obtained here is not possible, although the wave-front structure function is very similar to that obtained from the Zernike polynomials compensation.⁷ This fact suggests that the fundamental conclusions of this paper can be applied to actual systems, but a more detailed analysis is required for each particular case.

Uncompensated wave fronts can be characterized with use of the Fried parameter r_0 , which corresponds to the diameter of the atmospheric coherence area. In an equivalent way, it is possible to define a generalized Fried parameter ρ_0 corresponding to compensated wave fronts.

A relationship among ρ_0 , the correlation length, and the residual phase variance after compensation is introduced. From it, it is possible to derive an *a priori* estimate of ρ_0 , in terms of the number of corrected polynomials and the Fried parameter r_0 .

Using ρ_0 and the residual phase variance, we will describe the phase structure function, estimate the point-spread function (PSF) halo size, and derive an expression for the Strehl ratio. In contrast to other methods,⁸⁻¹⁰ this procedure is applicable to any degree of correction. This expression for the Strehl ratio can also be obtained from a generalization of Goodman's model for speckle.¹¹ The advantage of this model is that it provides, from the residual phase variance and ρ_0 , the statistics of the light intensity at the image plane.¹² Furthermore, we will demonstrate that ρ_0 represents the diameter of the coherent cells in Goodman's model. Theoretical developments for the correlation length, the generalized Fried parameter, the PSF halo width, and the Strehl ratio are checked with a standard simulation procedure to obtain the structure function and the light intensity distribution at the image plane as a function of the compensation. It is shown that results remain valid even when a limited level of noise is involved in the compensation process.

Thus the introduction of the generalized Fried parameter makes it easier to understand the physics underlying the image-formation process after atmospheric degradation and adaptive optics compensation, by analogy with the uncompensated case. Furthermore, some interesting conclusions can be derived that may be useful for developing procedures to calibrate adaptive optics systems or improving detection techniques.

2. GENERALIZED FRIED PARAMETER

This section describes the wave-front decomposition into Zernike polynomials, the phase structure function of the

wave front, the generalization of the Fried parameter, and the behavior of the phase correlation length.

A. Wave-Front Description

Optical wave fronts are two-dimensional functions that can be decomposed into Zernike polynomials that are separable in angle and radius and form an orthogonal basis. We will use the definition given by Noll,¹³

$$\phi(r, \theta) = \sum_{i=1}^{\infty} a_i Z_i(r, \theta), \quad (1)$$

where a_i are the coefficients of the corresponding Zernike polynomials (Z_i). The effect of partial compensation on the wave front is that some of the decomposition coefficients vanish. The residual distortion in the compensated wave front may be estimated with the Noll expression for the average variance over the wave-front surface once the first j Zernike terms have been corrected,

$$\Delta_j = \sum_{i=j+1}^{\infty} \langle |a_i|^2 \rangle = \text{coef}(j) \left(\frac{D}{r_0} \right)^{5/3}, \quad (2)$$

where $\langle \dots \rangle$ denotes an ensemble average and $\text{coef}(j)$ is the corresponding coefficient given by Noll.

B. Structure Function

The phase structure function is defined as

$$D_{\phi}(\mathbf{r} - \mathbf{r}') = \langle [\phi(\mathbf{r}) - \phi(\mathbf{r}')]^2 \rangle. \quad (3)$$

For apertures larger than 1 m, even in the best seeing sites, the phase fluctuation has a Gaussian distribution because of the central limit theorem. Its mean value is zero, and hence it is fully described by its second moment. The fact that the structure function is the second moment for differential phase fluctuation completely specifies the spatial statistics of phase fluctuation. Based on the Kolmogorov¹⁴ theory of turbulence, it is possible to show that in the absence of compensation the phase structure function may be written as

$$D_{\phi}(r) = 6.88 \left(\frac{r}{r_0} \right)^{5/3}, \quad (4)$$

where r_0 is the Fried parameter¹⁵ and $r = |\mathbf{r}|$. After compensation, the corrected wave front is no longer spatially stationary, and consequently the structure function depends on both \mathbf{r} and \mathbf{r}' . However, when the compensation increases, the wave front tends very quickly to be spatially stationary,^{16,17} and an average phase structure function can be defined, as is shown in Eq. (25). Now we consider the next approximated expression,

$$D_{\phi}(r) = 2\Delta_j \left[1 - \frac{\langle \phi(r')\phi(r+r') \rangle}{\Delta_j} \right] = 2\Delta_j [1 - \gamma(r)], \quad (5)$$

where $\gamma(r)$ is the normalized phase autocorrelation function. This approximation is more precise for a high degree of correction or large separation between points.

It is known¹⁸ that the shape of the structure function varies as a function of the degree of the compensation. As the separation between points becomes arbitrarily large, the autocorrelation function tends to zero and the

structure function saturates to $2\Delta_j$. However, for small separation distances the curve still follows the 5/3 power law^{7,19} and can be fitted by use of the following expression,

$$D_{\phi}(r) = 6.88 \left(\frac{r}{\rho_0} \right)^{5/3}, \quad (6)$$

where the value of the parameter ρ_0 varies as a function of the degree of compensation. This behavior suggests that ρ_0 is equivalent to the Fried parameter but corresponds to partially compensated wave fronts. We denote ρ_0 as the generalized Fried parameter. This analogy will lead us to several interesting results in the following sections.

C. Correlation Length

The phase correlation length in the wave front, l_{corr} , can be obtained from the structure function.²⁰ It is defined as the distance value for which the structure function leaves the 5/3 power behavior and reaches the constant value $2\Delta_j$. In this point it is fulfilled that

$$6.88 \left(\frac{l_{\text{corr}}}{\rho_0} \right)^{5/3} = 2\Delta_j. \quad (7)$$

It is interesting to note that the parameters Δ_j and ρ_0 are determined by the number of corrected polynomials and by the value of the ratio D/r_0 . However, the correlation length l_{corr} is completely determined by the number of corrected polynomials (in D units), as can be deduced from previous studies.²⁰ In Section 5 we obtain a fitting of the correlation length as a function of the number of corrected polynomials, which remains valid independently of the value of D/r_0 . Hence the generalized Fried parameter can be theoretically obtained from l_{corr} and Δ_j , i.e., from the number of corrected polynomials and the ratio D/r_0 .

3. STREHL RATIO FROM GENERALIZED GOODMAN'S MODEL

The image-formation process for speckle proposed by Goodman¹¹ has recently been generalized to the case of partially compensated images.^{12,21} An essential modification is introduced in Goodman's model. The phase distribution is no longer uniform in the interval $(-\pi, \pi)$ after compensation but becomes a Gaussian distribution of variance Δ_j . In this section we use this model to obtain the Strehl ratio; in Section 4 this expression will be compared with another one derived from the analysis of the PSF halo, and we will demonstrate that the size of the coherent cells in this model is described by the generalized Fried parameter.

The light intensity at the PSF core is obtained from the complex amplitude of the field at this point, which results from the sum of contributions from many elementary areas (cells) in the wave front. As an approximation, let the phase screen consist of coherent and independent correlation cells of diameter ρ . The number of these cells is then proportional to $(D/\rho)^2$. We can consider that each cell contributes a phasor whose amplitude is proportional

to the cell area. We assume that, in partially corrected wave fronts, these phasors fulfill the following conditions:

1. Amplitude and phase of elementary phasor are independent of each other and independent of amplitudes and phases of any other cell.

2. The phase distribution function is assumed to be a zero-mean Gaussian function of variance Δ_j that decreases when the number of corrected polynomials increases:

$$P(\phi) = \left(\frac{1}{2\pi\Delta_j} \right)^{1/2} \exp\left(-\frac{\phi^2}{2\Delta_j}\right). \quad (8)$$

The variance Δ_j can be directly determined from Noll's expression, Eq. (2), once the degree of compensation to be performed has been determined.

The characteristic function corresponding to the probability density function of the phase, $M_\phi(\omega)$, can be evaluated as its Fourier transform:

$$M_\phi(\omega) = \int_{-\infty}^{\infty} \exp(j\omega\phi)P(\phi)d\phi = \exp\left(-\frac{\Delta_j\omega^2}{2}\right). \quad (9)$$

Let A_r and A_i be the real and the imaginary parts of the resultant field at the central point of the image plane defined by

$$A_r = \frac{1}{\sqrt{N}} \sum_{k=1}^N |\alpha_k| \cos \phi_k, \\ A_i = \frac{1}{\sqrt{N}} \sum_{k=1}^N |\alpha_k| \sin \phi_k, \quad (10)$$

where N is the number of independent cells, α_k/\sqrt{N} the amplitude, and ϕ_k the phase of the k th elementary phasor. The mean and the variance of both the real and the imaginary parts can be obtained from the phase characteristic function¹¹:

$$\langle A_r \rangle = \bar{\alpha} M_\phi(1) \sqrt{N}, \quad \langle A_i \rangle = 0, \\ \sigma_r^2 = \frac{\overline{\alpha^2}}{2} [1 + M_\phi(2)] - (\bar{\alpha})^2 M_\phi^2(1), \\ \sigma_i^2 = \frac{\overline{\alpha^2}}{2} [1 - M_\phi(2)]. \quad (11)$$

From now on we will assume that $\overline{\alpha^2} = (\bar{\alpha})^2 = \overline{(\alpha_k)^2}$, since we are not considering scintillation. The energy incoming at the PSF core can be expressed as

$$\langle E \rangle = \langle A_r \rangle^2 + \sigma_r^2 + \langle A_i \rangle^2 + \sigma_i^2 \\ = [1 + (N-1)\exp(-\Delta_j)](\bar{\alpha})^2. \quad (12)$$

The core intensity will then be $\langle I \rangle = \langle E \rangle / a_{\text{core}}$, where

$$a_{\text{core}} = \pi \left(\frac{\lambda f}{2D} \right)^2 \quad (13)$$

is the minimum area obtainable from a diffraction-limited telescope.

The Strehl ratio is the ratio between the energies at the core with and without turbulence. With Eq. (12) and taking into account that in the absence of turbulence $\Delta_j = 0$,

$$SR = \frac{[1 + (N-1)\exp(-\Delta_j)]}{N}. \quad (14)$$

Finally, we note that this model can also provide the light intensity statistics^{12,21} and the photon statistics²² at the image plane. The *a priori* knowledge of the light intensity statistics at the image plane can be a useful tool in analyzing the system behavior.

4. STREHL RATIO FROM THE HALO ANALYSIS

In this section the Strehl ratio is obtained from the halo analysis and is compared with that derived in Section 3. We demonstrate that the size of the coherent cells in the compensated wave front is described by the generalized Fried parameter.

The Fried parameter gives a measure of the maximum resolution attainable in uncompensated long-exposure images. Thus the PSF size is proportional to λ/r_0 . As compensation increases, the image becomes a bright core surrounded by a speckled halo.^{11,19,23} The halo width (ω_0) can be obtained [equivalently to Eq. (7.20) in Ref. 24] from

$$\int_{\text{image}} I_{\text{halo}}(\mathbf{x}) d\mathbf{x} = \frac{\pi}{4} \omega_0^2 I_{\text{halo}}(\mathbf{0}). \quad (15)$$

The left-hand side of Eq. (15) is the total energy at the halo. To estimate its value, we will use the expression of the structure function shown in Section 2. From Eq. (5) an approximated expression for the optical transfer function (OTF) can be found:

$$\text{OTF} = \text{OTF}_{\text{TEL}} \exp(-D_{\phi/2}) \\ = \text{OTF}_{\text{TEL}} \exp[-\Delta_j(1 - \gamma)] \\ = \text{OTF}_{\text{TEL}} \{ \exp(-\Delta_j) + \exp(-\Delta_j)[\exp(\gamma\Delta_j) - 1] \}. \quad (16)$$

As the separation between points becomes arbitrarily large, the autocorrelation function tends to zero, and hence the first term is the asymptote to which the OTF falls, whereas the second represents the rise above that asymptote. Assuming that the OTF of the original telescope is much wider than the second term, an approximated expression for the PSF becomes

$$\text{PSF} = \text{PSF}_{\text{TEL}} \exp(-\Delta_j) \\ + \text{FT}\{ \exp(-\Delta_j)[\exp(\gamma\Delta_j) - 1] \}. \quad (17)$$

The first term (coherent energy) can be interpreted as a diffraction-limited core of the PSF and the second as a much broader halo. Thus the coherent energy is approximately a fraction $\exp(-\Delta_j)$ of the total energy, and, consequently, the total energy in the halo is $[1 - \exp(-\Delta_j)]$ times the total energy, E_T .

Then the first term of Eq. (15) can be estimated as

$$\int_{\text{image}} I_{\text{halo}}(\mathbf{x}) d\mathbf{x} = E_T [1 - \exp(-\Delta_j)]. \quad (18)$$

On the other hand, $\omega_0 = (\lambda f/2\rho_0)$ is the average diameter of the halo (where f is the focal length of the system) and $I_{\text{halo}}(\mathbf{0})$ is the intensity of the halo at the core and can be estimated from the difference between the total intensity at the core $[I(\mathbf{0})]$ and the coherent intensity at the core $[I_C(\mathbf{0})]$. The total and coherent energy at the core can be calculated by multiplying these intensities by the core area:

$$\begin{aligned} E(\mathbf{0}) &= I(\mathbf{0}) \pi \left(\frac{\lambda f}{2D} \right)^2, \\ E_C(\mathbf{0}) &= I_C(\mathbf{0}) \pi \left(\frac{\lambda f}{2D} \right)^2. \end{aligned} \quad (19)$$

After these considerations Eq. (15) can now be written as

$$E_i [1 - \exp(-\Delta_j)] = \frac{\pi(\lambda f/2\rho_0)^2}{\pi(\lambda f/2D)^2} [E(\mathbf{0}) - E_C(\mathbf{0})] \quad (20)$$

from this expression and, considering that all the coherent energy is at the PSF core, $E_c(\mathbf{0}) = E_T \exp(-\Delta_j)$, the energy at the image core will be

$$E(\mathbf{0}) = \frac{E_T}{(D/\rho_0)^2} \{1 + [(D/\rho_0)^2 - 1] \exp(-\Delta_j)\}, \quad (21)$$

where $(D/\rho_0)^2$ is the number of speckles in the image. Thus the Strehl ratio is

$$\text{SR} = \frac{1}{(D/\rho_0)^2} \{1 + [(D/\rho_0)^2 - 1] \exp(-\Delta_j)\}. \quad (22)$$

If we compare Eq. (22) with Eq. (14), we realize that the number of coherent cells N is equal to $(D/\rho_0)^2$. Hence

$$D_{\phi}(\mathbf{r}) = \frac{\left\langle \int [\phi^2(\mathbf{r}') + \phi^2(\mathbf{r}' + \mathbf{r})] P(\mathbf{r}') P(\mathbf{r}' + \mathbf{r}) d\mathbf{r}' - 2 \int \phi(\mathbf{r}') \phi(\mathbf{r}' + \mathbf{r}) P(\mathbf{r}') P(\mathbf{r}' + \mathbf{r}) d\mathbf{r}' \right\rangle}{\int P(\mathbf{r}') P(\mathbf{r}' + \mathbf{r}) d\mathbf{r}'}, \quad (25)$$

the generalized Fried parameter $\rho_0 = \rho$ represents the diameter of the coherent cells in Goodman's model, as could have been expected from the analogy with the Fried parameter r_0 , which is sometimes called the seeing cell size.

A similar result is obtained by Hardy¹⁹ from the analysis of the Strehl ratio in the halo, although he uses an approximated expression given by Yura²⁵ to estimate the peak intensity at the halo and does not consider the evolution of the Fried parameter with compensation. It is interesting to state that we have obtained two identical expressions for the Strehl ratio with two completely different methods. One is based on the wave-front distribution explained in the generalized Goodman model, whereas the other relies on the structure function analysis.

Two special cases can be considered. In the case of low compensation (large values of Δ_j), the value of $\exp(-\Delta_j)$ can be neglected and

$$\text{SR} \approx \frac{1}{N} = \left(\frac{\rho_0}{D} \right)^2 \approx \left(\frac{r_0}{D} \right)^2. \quad (23)$$

That is, there is no contribution from the peak of the PSF, and the whole image is speckled. On the other hand, for a large number of corrected polynomials and taking into account that $\rho_0 < D$, we can obtain

$$\text{SR} \approx \exp(-\Delta_j). \quad (24)$$

Then most of the incoming energy comes to the peak of the PSF, and no energy is directed to the surrounding halo. This expression is the same as that derived from diffraction theory⁸ for a high degree of compensation.

Hence a procedure to obtain the Strehl ratio from the number of corrected polynomials and the ratio D/r_0 has been developed. It has the advantage that it is applicable in any degree of compensation, in contrast to other methods.⁸⁻¹⁰

5. SIMULATION AND DISCUSSION

A. Simulation Procedure

To generate the phase structure function and to check the theoretical models introduced throughout the paper, we use a standard procedure to simulate wave fronts with different degrees of compensation proposed by Roddier.¹⁸ It is assumed that the atmosphere, which follows a Kolmogorov power spectrum, produces changes only in the phase of the electromagnetic field; scintillation is neglected. The wave front is decomposed into Zernike polynomials that allows us to control the degree of correction. Wave fronts are simulated with 560 Zernike polynomials. The number of samples in the entrance pupil is 128×128 . The phase structure function is calculated from the simulated wave fronts using the following expression,

where $P(\mathbf{r})$ is the pupil entrance function, which is equal to 1 inside the pupil and zero outside it. The first integral in the numerator is twice the correlation between $\phi^2(\mathbf{r})$ and $P(\mathbf{r})$, the second one is twice the autocorrelation of $[P(\mathbf{r})\phi(\mathbf{r})]$, and the denominator is the autocorrelation of $P(\mathbf{r})$. All these terms are easily calculated by use of the Fourier transform properties. The structure functions are obtained after averaging a series of 10^4 frames.

The light intensity long-exposure PSF for the different degrees of compensation is obtained from the squared modulus of the Fourier transform of the field at the entrance pupil:

$$\text{PSF}(\mathbf{x}) = \langle |\text{FT}\{P(\mathbf{r}) \exp[i\phi(\mathbf{r})]\}|^2 \rangle. \quad (26)$$

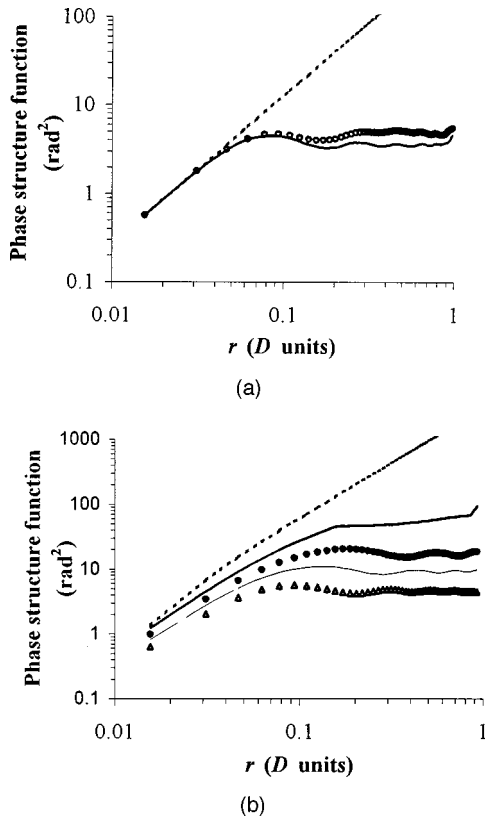


Fig. 1. (a) Structure function of the wave-front phase for $D/r_0 = 38.4$ and 100 (solid curve) corrected polynomials, assuming perfect compensation. It is compared with the structure function with 100 compensated polynomials when each coefficient is affected by a 10% error (circles). Dashed curve, reference line with a 5/3 slope. (b) Structure function of the wave-front phase for $D/r_0 = 38.4$ and 1 (short-dashed curve), 6 (solid curve), 21 (circles), 41 (long-dashed curve), and 81 (triangles) corrected polynomials.

Furthermore, the light intensity is also obtained by averaging a series of 10^4 experiments.

To check the effect of the noise involved in the compensation process on the behavior of the structure function, we analyzed several cases. Figure 1(a) shows the structure function for 100 corrected polynomials (solid curve) and $D/r_0 = 38.4$. This curve was obtained by assuming that no error is involved in the compensation process. It is compared with the structure function after compensation of 100 coefficients when each coefficient is affected by a 10% error (circles). The two curves are very close and follow a 5/3 power law for small values of r , so that the value of ρ_0 is the same in both cases. Furthermore, Eq. (7) can be used to obtain an estimate of the correlation length (l_{corr}), providing good results when the theoretical residual phase variance is used. This behavior corresponding to 100 corrected polynomials was also obtained for a wide range of compensation levels. Hence results obtained by simulating compensated wave fronts by assigning a zero value to the Zernike coefficients can be applicable to systems affected by limited noise.

B. Correlation Length Fitting

Using the simulation procedure stated in Eq. (25), we obtained the structure function for different degrees of com-

ensation. Figure 1(b) shows the structure function $D_\phi(r)$ for uncompensated wave fronts (short-dashed curve), which follows a 5/3 power law. The structure function for 6 (solid curve), 21 (circles), 41 (long-dashed curve), and 81 (triangles) corrected polynomials are also included. It can be seen that in corrected wave fronts the structure function follows a 5/3 power law for distances smaller than the correlation length and saturates to the $2\Delta_j$ value that can be estimated with Eq. (2). Thus for small spatial distances the only effect of compensation is to increase the generalized Fried parameter.

From the analysis of the structure function it is possible to obtain the value of the correlation length as a function of the degree of compensation. Figure 2 shows the evolution of l_{corr} as a function of the degree of compensation. When the number of corrected polynomials increases, the value of l_{corr} decreases. This behavior does not depend on the initial value of r_0 but rather only on the value of the telescope diameter D and on the number of corrected polynomials. This can be seen in Fig. 2, where the series corresponding to $r_0 = 1$ matches that of $r_0 = 1/38.4$, both with the same value of D . Then the behavior of l_{corr} can be described by a generic curve fitted to the values of l_{corr} obtained from the simulated structure functions. The fitted curve is given by

$$l_{\text{corr}} \approx 0.286j^{-0.362}D, \quad (27)$$

where j is the number of corrected polynomials.

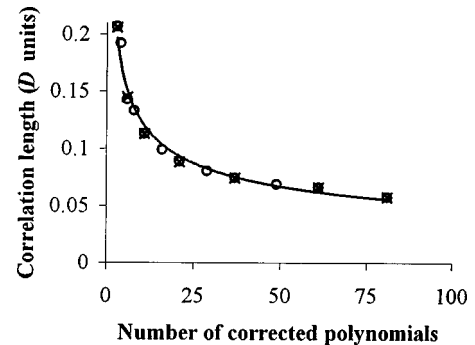


Fig. 2. Correlation length values obtained from the structure function series for $r_0 = 1/38.4$ (circles), for $r_0 = 1$ (crosses), and for values of the fitting curve expressed by Eq. (27) (solid curve) as a function of the number of corrected polynomials.

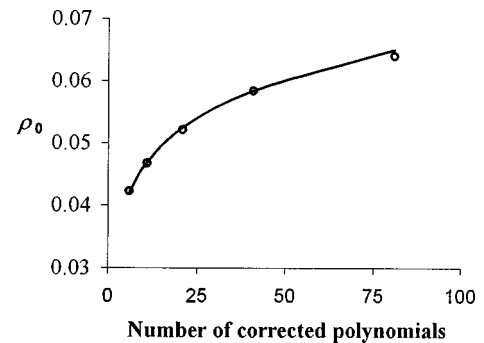


Fig. 3. Value of ρ_0 in the compensated wave front as a function of the number of corrected polynomials for $D/r_0 = 38.4$. Solid curve, values obtained from Eq. (28); circles, values obtained from the fitting of the structure function.

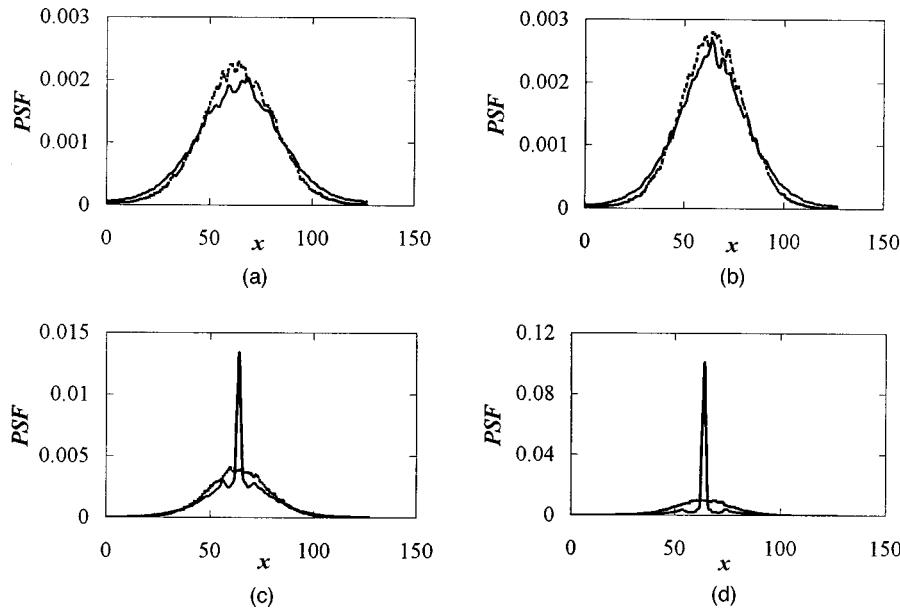


Fig. 4. Solid curves, cross sections of the simulated PSF for a fixed value of $D/r_0 = 38.4$ and (a) 11, (b) 21, (c) 41, and (d) 81 corrected polynomials. Dashed curves, cross section of PSF simulated with no compensation and a value $D/r_0 = D/\rho_0$, where ρ_0 is obtained from Eq. (28) with $r_0 = 1/38.4$ and $j =$ (a)11, (b) 21, (c) 41, and (d) 81 corrected polynomials.

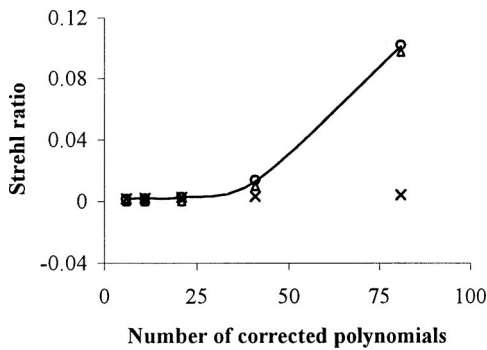


Fig. 5. Strehl ratio from simulated images (circles) compared with the theoretical values obtained from Eq. (22) (solid curve) [where ρ_0 is estimated from Eq. (28)] and with approximated values obtained from Eq. (23) (crosses) and Eq. (24) (triangles).

C. PSF Analysis

Consequently, from the telescope diameter, the Fried parameter, and the number of corrected polynomials, we can estimate the average phase variance and the correlation length using Eqs. (2) and (27), respectively. Then from Eq. (7) we can derive the generalized Fried parameter:

$$\rho_0 = \left(\frac{3.44}{\Delta_j} \right)^{3/5} l_{\text{corr}} = \left(\frac{3.44}{\text{coef}(j)} \right)^{3/5} 0.286j^{-0.362}r_0. \quad (28)$$

It is important to note that the improvement in the halo resolution, described by the ratio ρ_0/r_0 , depends only on the number of corrected polynomials.

It is possible to fit the simulated structure function for distances smaller than the correlation length with the theoretical expression given by Eq. (6) so that values of ρ_0 are obtained as a function of the degree of compensation. Figure 3 shows a series of values of ρ_0 obtained from the fitting of the structure function together with those obtained with Eq. (28). It can be seen that the two series of data fit quite well.

Now we will verify that the generalized Fried parameter gives the halo width. Figure 4 shows simulated PSF's for a fixed value of $D/r_0 = 38.4$ and different levels of compensation: 11, 21, 41, and 81 corrected polynomials (solid curves). For each compensation level a halo of width λ/ρ_0 (dashed curves) is also included [this PSF of width λ/ρ_0 is obtained by simulating uncompensated wave fronts with $D/r_0 = D/\rho_0$, where ρ_0 is given by Eq. (28)]. It is possible to see that the width of the halo in the first series of PSF's is similar to that of the second series. This allows us to state that the value of ρ_0 obtained from the fitting of the structure function is inversely proportional to the halo width. For a low number of corrected polynomials, when the bright core cannot be distinguished from the speckled halo, the two PSF's are the same, and hence the effect of compensation is just a decrease in the ratio between the telescope diameter and the Fried parameter. In this case, the improvement in image resolution is inversely proportional to $j^{0.362} \cdot \text{coef}(j)^{0.6}$. For higher degrees of correction the coherent peak emerges from the speckled halo as predicted by Eq. (17).

The Strehl ratio from simulated images (circles) is shown in Fig. 5. It is compared with values obtained from Eq. (22), where ρ_0 is estimated from Eq. (28) (solid curve). There is a good fit between theoretical and simulated values for the whole range of corrected polynomials even when other approximated estimates fail. This confirms the validity of our method. Furthermore, the approximation stated in Eq. (23) behaves well in low compensation. Finally, we verify that our expression tends to a well-known result from diffraction theory, Eq. (24), for a great number of corrected polynomials. Our method has the advantage that it is applicable for any degree of correction. To make this more evident, Fig. 6 shows the relative error in the estimation of the Strehl ra-

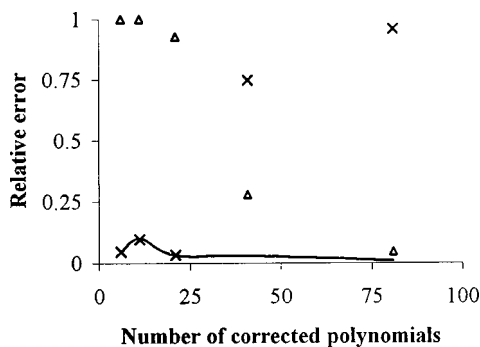


Fig. 6. Relative error in the estimation of the Strehl ratio from the theoretical expression given by Eq. (22) (solid curve) [where ρ_0 is estimated from Eq. (28)] and from the approximated expressions given by Eq. (23) (crosses), and Eq. (24) (triangles).

tio. The Strehl ratio relative error with Eq. (22) (solid curve) is compared with those obtained from approximated expressions given by Eq. (23) (crosses) and Eq. (24) (triangles). While Eqs. (23) and (24) behave well only for low and high compensation, respectively, Eq. (22) gives an accurate estimate of the Strehl ratio for the whole range of corrected polynomials.

6. CONCLUSIONS

A series of concepts involved in the image-formation process when partial compensation with an adaptive optics system is performed over a wave front has been developed. By analogy with the Fried parameter, r_0 , we have introduced a generalized Fried parameter, ρ_0 , that plays the same role as r_0 but in partial compensation. Using this parameter and the residual phase variance, we have described the phase structure function, estimated the point-spread function halo size, and derived an expression for the Strehl ratio. In contrast to other methods, this procedure is applicable to any degree of correction.

This expression for the Strehl ratio can also be obtained from a generalization of Goodman's theory for speckle; in this case, ρ_0 represents the diameter of the coherent cells. This model provides, from the residual phase variance and ρ_0 , the statistics of the light intensity in the image plane. The *a priori* knowledge of the light intensity statistics at the image plane may allow the development of procedures to improve the image analysis or the system calibration.

We have obtained an expression for the correlation length in terms of the number of corrected polynomials, provided that the correlation length does not depend on the atmospheric conditions but only on the degree of compensation and the telescope diameter. As a result, we have seen how the value of ρ_0 increases and the correlation length decreases with compensation. This information may be used as a way to calibrate the accuracy of the adaptive optics system.

Results were checked with a standard simulation technique based on a perfect compensation of Zernike polynomials because of the limited effect of noise involved in compensation on the wave-front structure function. The fairly good fit between theoretical and simulated values

confirms that the models used in the theoretical development work properly at least to perform this sort of analysis.

ACKNOWLEDGMENT

This work has been supported by the Dirección General de Enseñanza Superior e Investigación Científica under project PB97-0355.

M. Cagigal can be reached at the address on the title page or by e-mail at mpc@opt.unican.es.

REFERENCES

1. J. Y. Wang and J. K. Markey, "Modal compensation of atmospheric turbulence phase distortion," *J. Opt. Soc. Am.* **68**, 78–87 (1978).
2. F. Rigaut, G. Rousset, J. C. Fontanella, J. P. Gaffard, F. Merkle, and P. Lena, "Adaptive optics on a 3.6-m telescope: results and performance," *Astron. Astrophys.* **250**, 280–290 (1991).
3. M. C. Roggemann, "Limited degree-of-freedom adaptive optics and image reconstruction," *Appl. Opt.* **30**, 4227–4233 (1991).
4. M. C. Roggemann and B. Welsh, *Imaging through Turbulence* (CRC Press, Boca Raton, Fla., 1996).
5. A. Glindemann, "Improved performance of adaptive optics in the visible," *J. Opt. Soc. Am. A* **11**, 1370–1375 (1994).
6. P. Nisenson and R. Barakat, "Partial atmospheric correction with adaptive optics," *J. Opt. Soc. Am. A* **4**, 2249–2253 (1987).
7. F. Rigaut, B. L. Ellerbroek, and M. J. Northcott, "Comparison of curvature-based and Shack–Hartmann-based adaptive optics for the Gemini telescope," *Appl. Opt.* **36**, 2856–2868 (1997).
8. M. Born and E. Wolf, *Principles of Optics* (Pergamon, Oxford, UK, 1993).
9. G. Valley, "Long- and short-term Strehl ratios for turbulence with finite inner and outer scales," *Appl. Opt.* **18**, 984–987 (1979).
10. J. Winocur, "Modal compensation of atmospheric turbulence induced wave front aberrations," *Appl. Opt.* **21**, 433–438 (1982).
11. J. W. Goodman, *Statistical Optics* (Wiley-Interscience, New York, 1985).
12. V. F. Canales and M. P. Cagigal, "Rician distribution to describe speckle statistics in adaptive optics partial correction," *Appl. Opt.* **38**, 766–771 (1999).
13. R. J. Noll, "Zernike polynomials and atmospheric turbulence," *J. Opt. Soc. Am.* **66**, 207–211 (1976).
14. A. Kolmogorov, *Classic Papers on Statistical Theory*, S. Friedlander and L. Topper, eds. (Interscience, New York, 1961).
15. D. L. Fried, "Statistics for a geometric representation of wavefront distortion," *J. Opt. Soc. Am.* **55**, 1427–1435 (1965).
16. J. Conan, "Etude de la correction partielle en optique adaptative," Ph.D. dissertation, Office National d'Etudes et de Recherches Aérospatiales Pub. 1995-1 (Paris, 1995).
17. M. P. Cagigal and V. F. Canales, "Analysis of the photon statistics in partially corrected wavefronts," in *Propagation and Imaging through the Atmosphere*, L. R. Bissonnette and C. Dainty, eds., *Proc. SPIE* **3125**, 320–326 (1997).
18. N. Roddier, "Atmospheric wavefront simulation using Zernike polynomials," *Opt. Eng.* **29**, 1174–1180 (1990).
19. J. W. Hardy, *Adaptive Optics for Astronomical Telescopes* (Oxford U. Press, Oxford, UK, 1998).
20. G. Valley and S. Wandzura, "Spatial correlation of phase

- expansion coefficients for propagation through atmospheric turbulence," *J. Opt. Soc. Am.* **69**, 712–717 (1979).
21. M. P. Cagigal and V. F. Canales, "Speckle statistics in partially corrected wave fronts," *Opt. Lett.* **23**, 1072–1074 (1998).
 22. V. F. Canales and M. P. Cagigal, "Photon statistics in partially compensated wave fronts," *J. Opt. Soc. Am. A* **16**, 2550–2554 (1999).
 23. R. Smithson, M. Peri, and R. Benson, "Quantitative simulation of image correction for astronomy with a segmented mirror," *Appl. Opt.* **27**, 1615–1620 (1988).
 24. F. Roddier, "The effects of atmospheric turbulence in optical astronomy," in *Progress in Optics XIX*, E. Wolf, ed., (North-Holland, Amsterdam, 1981), pp. 281–376.
 25. H. T. Yura, "Short-term average optical beam spread in a turbulent medium," *J. Opt. Soc. Am.* **63**, 567–572 (1973).